# On the Wavelength-Dependent Performance of Cr-Doped Silica in Selective Photo-Oxidation

**Otto Berg,*,† Mohamed S. Hamdy,‡ Thomas Maschmeyer,§ Jacob A. Moulijn,‡ Mischa Bonn,†,|| and Guido Mul‡**

*Leiden Institute of Chemistry, Leiden University, Einsteinweg 55, P.O. Box 9502, 2300 RA Leiden, The Netherlands, Reactor and Catalysis Engineering, DelftChemTech, Technische Universiteit Delft, Julianalaan 136, 2628 BL, Delft, The Netherlands, Laboratory of Advanced Catalysis for Sustainability, School of Chemistry, The University of Sydney, NSW 2006, Australia, and FOM-Institute for Atomic and Molecular Physics AMOLF, Kruislaan 407, 1098 SJ Amsterdam, The Netherlands*

*Received: July 16, 2007; In Final Form: November 13, 2007*

We have evaluated the hypothesis that the performance of a chromium-based photocatalyst (activity and selectivity) can be tuned by means of the wavelength to which the catalyst is exposed. To this end, we synthesized an amorphous, mesoporous silica matrix loaded with 10 at % chromium/silicon, characterized its structure, and tested its performance in selective oxidation of propane to acetone. Spectroscopy, microscopy, and X-ray diffraction show that chromium is present in this catalyst as both isolated Cr(VI) sites and crystalline Cr(III) oxide. The photochemical reaction rate depends strongly on excitation wavelength in the range of 300−700 nm, with a well-resolved maximum at 460 nm. At this wavelength, adsorbed acetone is produced with approximately 60% selectivity over carboxylates. Only very minor variations in selectivity were observed over the same range of wavelengths. By comparison of absorbance, luminescence, and reaction−excitation spectra we are able to identify the photoactivated catalytic site as an excited state of isolated Cr(VI) oxide in tetrahedral coordination. Therefore a heterogeneity of chemical structure, which is correlated with heterogeneity of an unresolved absorption spectrum, can be the basis of wavelength-dependent photocatalytic activity.

## Introduction

Many studies of photocatalysis have been directed toward environmental applications, such as the possibility of ambient water and air purification. Also of interest, from a chemical-synthetic perspective, is the use of light to perform difficult selective oxidation reactions.[1] Extremely high selectivities have been observed within cation-exchanged zeolites, where a transient adsorbate/cation complex is believed to absorb light.[2] However, quantitative and complete catalytic cycles have not been obtained with these systems. An alternative is to employ solids with intrinsic absorption bands of suitable energy. Transition-metal oxides absorb light at visible frequencies, and in some cases this energy can be used to activate C−H bonds in saturated hydrocarbons—a chemical step that is generally inefficient and unselective. In particular Anpo and co-workers have documented the photocatalytic properties of chromium doped into various mesoporous materials, including the silicate HMS[3,4] and zeolite ZSM-5.[5]

We have recently developed a form of mesoporous amorphous silica (TUD-1) as a matrix for photocatalytic chromophores such as chromium[6] and titanium[7] oxides and have demonstrated that these composite materials photo-oxidize propane to acetone with good selectivity. Our previous report on Cr-doped TUD-1 documented the photochemical activity and selectivity under 435-nm illumination only. Here we compare the wavelength dependence of light absorption, re-emission, and propane photo-oxidation rate. The catalyst under study contains chromium in various states of dispersion and oxidation, which together yield broad and poorly resolved absorption features. In contrast, the reaction−excitation spectrum shows a well-resolved peak; it corresponds to the absorption of isolated Cr(VI) oxide, as observed by fluorescence excitation. Although used here as a method to identify the active site, similar optical-spectroscopic methods could perhaps be used to optimize practical reactions.

## Methods

In a typical Cr TUD-1 synthesis, a mixture of triethanolamine (TEA, 97%, ACROS) and deionized water was added dropwise to a solution of tetraethylorthosilicate (TEOS, 98+%, ACROS) and chromium salt ($CrNO_3 \cdot 9H_2O$, 99%, Aldrich) in 5 mL of deionized water, while stirring. Thereafter tetraethyl ammonium hydroxide (TEAOH, 35%, Aldrich) was added. This mixture was aged for 24 h under atmospheric conditions, dried for 24 h at 371 K, hydrothermally treated at 455 K for 8 h, and calcined at 873 K for 10 h (additional details are published elsewhere[6]). The final product was a green powder. The synthesis mixture for Cr-10 TUD-1 had a molar composition of 1 $SiO_2$:0.1$Cr_2O_3$:0.3 TEAOH:1 TEA:11 $H_2O$. Elemental analysis of the final product by neutron activation analysis yielded a Si/Cr ratio of 9.8, as expected. X-ray diffraction patterns were recorded using Cu K$\alpha$ radiation on a Philips PW 1840 diffractometer equipped with a graphite monochromator. The samples were scanned through the range 0.1−80° 2$\theta$ in steps of 0.02°. Nitrogen adsorption isotherms were recorded on a Quantachrome Autosorb-6B at 77 K. The adsorption branch was converted to a

* To whom correspondence should be addressed. E-mail: o.berg@chem.leidenuniv.nl. Fax: (+31) 71 527-4452. Tel: (+31) 71 527-4451.
† University of Leiden.
‡ Technische Universiteit Delft.
§ The University of Sydney.
|| AMOLF.

10.1021/jp075562k CCC: $40.75 
Published on Web 03/19/2008

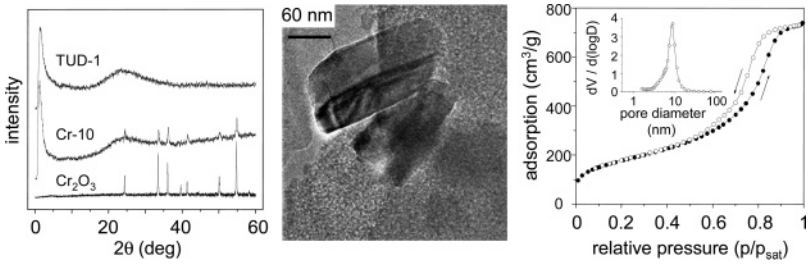


**Figure 1.** Physical characterization of the Cr-10 TUD-1 sample. Left: powder X-ray diffraction patterns of the matrix material, the Cr-loaded composite, and pure $Cr_2O_3$. Center: electron micrograph of typical $Cr_2O_3$ inclusions. Right: $N_2$ adsorption isotherm at 77 K, with a pore size distribution (inset) computed from the adsorption branch.

pore size distribution by means of the Barret−Joyner−Halenda model.[8] The specific surface area was obtained from a fit to the Brunauer−Emmett−Teller (BET) isotherm, while the pore volume was determined by the t-plot method.[9] Diffuse reflectance UV−vis spectra were recorded on a CaryWin 300 spectrometer using $BaSO_4$ as reference, under the same conditions as used for the photoactivity measurements.

Cr-10 TUD-1 wafers were formed on an automatic press (SPECTA) at 3 tons/cm$^2$. The samples were edge mounted on a copper sample holder equipped with a resistive heater and type K thermocouples. The holder was mounted in a stainless steel high vacuum chamber; $CaF_2$ windows were used for infrared spectroscopy and fused silica for luminescence. All samples were activated by ramping to 573 K at 15 K/min under high vacuum ($10^{-6}$ mbar) and dwelling for 20 min. After cooling to room temperature, the cell was loaded with 2.75 mbar of propane and 400 mbar of molecular oxygen. During irradiation, infrared spectra were obtained with a Bio-Rad 175 FTIR spectrophotometer operating at a resolution of 4 cm$^{-1}$. Absorbance, $A$, was calculated from the sample intensity, $I$, and reference intensity, $I_0$: $A = -\log_{10}(I/I_0)$. The product absorbance bands were deconvoluted into the sum of three Gaussian peaks and a linear baseline by means of a nonlinear least-squares fit. The concentration of product molecules was then calculated from the area of these Gaussian components by means of the Beer−Lambert law, integrated over frequency: $\tilde{A} = \tilde{\sigma} \times D/\ln(10)$. With integrated absorbance $\tilde{A}$ (cm$^{-1}$) and integrated cross section $\tilde{\sigma}$ (cm/molecule), $D$ is the radiometric "column density" of absorbing species normal to the infrared beam direction (molecules/cm$^2$, not to be confused with the coverage of the catalytic particles). Because the concentration of products may depend on depth from the irradiated surface, the data are not sufficient to calculate local concentrations. By use of integrated cross sections of $3.24 \times 10^{-17}$ cm/(acetone molecule) and $4.7 \times 10^{-17}$ cm/(carboxylate molecule),[10] the column density of products (moles /cm$^2$), when divided by the excitation fluence (J/cm$^2$), gives a measure of photochemical yield—reported here as $\mu$mol/(mW*h).

Three lamp systems were used, depending on the wavelength of interest: a 500-W capillary Hg arc (Philips SP500), a 250-W tungsten−halogen filament, and a 150-W Xe arc (Ushio UXL-151H in a PTI 1010B housing). The frequency was selected by means of a grating monochromator (Spex 0.2 m) with a bandpass of 7−12 nm and glass filters. Illumination power was measured with a thermopile meter (Scientech 360001) to a precision better than 10%; due to reflective losses, however, the absolute irradiance at the sample was less accurately known. Luminescence was induced by chopping the wavelength-selected light at 1200 Hz before the sample. Emission was collected at $f$/1.2 in the specular direction, at right angles to excitation. The light was filtered, dispersed with a grating monochromator (Spex 0.2 m), and detected with a red-sensitive photomultiplier tube (Burle 4840) and lock-in amplifier (PAR model 122). Spectral sensitivity was calibrated with respect to a 3400 K blackbody.

## Results and Discussion

**Physical Characterization.** TUD-1 is formed by sol-gel polymerization of an alkylsilane precursor, followed by calcination. Chemically the material is amorphous silica. Through the use of TEA as a templating agent, together with programmed hydrothermal treatment, its mesoscopic texture can be homogenized and controlled.[11] Both the uniformity and high connectivity of the resulting pore network are beneficial for photocatalytic applications. The one-pot surfactant-free synthesis allows for easy incorporation of transition metal dopants. At chromium/silicon concentrations of 1% or less, we find that chromium is incorporated in the form of isolated ions in the silica network. At higher concentrations polychromate entities $(O-Cr-O)_n$ are suspected, leading ultimately to crystalline chromium oxide inclusions. Some compositional details of the Cr-10 TUD-1 sample, which contains 10 at % Cr/Si, are shown in Figure 1. The left panel compares X-ray diffractograms of pure TUD-1, Cr-10 TUD-1, and polycrystalline $Cr_2O_3$. In the composite material sharp peaks diagnostic of $Cr_2O_3$ (25, 36, 41, 50, and 55° 2$\theta$) are superimposed on the diffuse peaks due to the glassy silica matrix. The central panel of Figure 1 is a transmission electron micrograph of the same material. Here crystalline $Cr_2O_3$ inclusions are visible against a stippled background of TUD-1. The depth of field obscures the mesostructure of the matrix, but this can be characterized by means of gas adsorption. An isotherm for $N_2$ at 77 K is shown in the right-hand panel. Hysteresis occurs during capillary condensation within the pores; that the adsorption and desorption branches are parallel is an indication of mesoscopic uniformity. When the same data are represented as a pore size distribution (inset) a narrow maximum is found at 9.1 nm. The specific surface area calculated from these data is 634 m$^2$/g, with a pore volume of 1.14 cm$^3$/g.

**Propane Oxidation.** Chromium-doped TUD-1 absorbs light throughout the visible spectrum, and this energy can sensitize reactions among molecules that are adsorbed within the mesopores. A useful assay of photocatalytic performance is the oxidation of propane. The desired partial-oxidation products, acetone and water, are easily distinguished from further-oxidized $C_3$ species (carboxylates) and the ultimate combustion product (carbon dioxide) by means of infrared spectroscopy. Therefore we use an FTIR spectrophotometer to observe the appearance of adsorbed reaction products during irradiation. The optical setup is shown schematically in Figure 2. With a broadband lamp and monochromator the excitation can be tuned throughout visible and near-ultraviolet wavelengths.

The upper panel of Figure 3 shows infrared spectra of adsorbed photochemical reaction products. The spectrum is

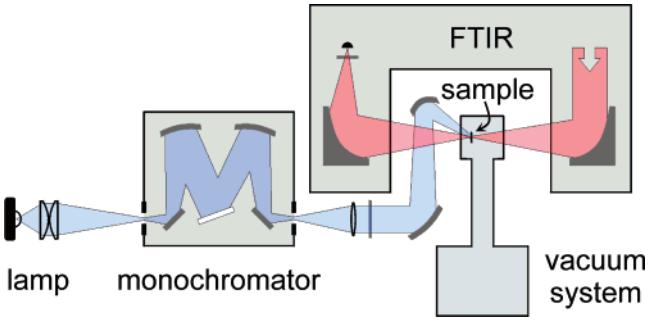


**Figure 2.** Schematic diagram of the optical layout for simultaneous dosing, irradiation, and infrared spectroscopy of catalyst wafers. The sample is irradiated with wavelength-selected visible light, and the vibrational spectra are obtained in transmission.

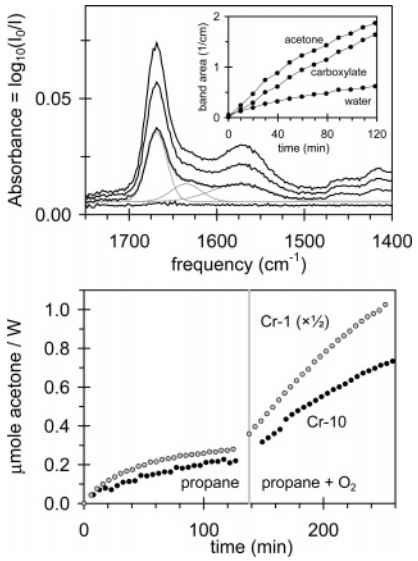


**Figure 3.** Evaluation of Cr TUD-1 as photocatalyst. Upper panel: characteristic infrared spectra of adsorbed products, obtained at 40-min intervals, in the presence of propane, oxygen, and blue light (430 nm, 17 mW/cm$^2$). Vibrations characteristic of acetone (1669 cm$^{-1}$), carboxylates (1573 cm$^{-1}$), and water (1635 cm$^{-1}$) are deconvoluted as shown for the 40-min spectrum. The growth of these components as a function of irradiation time is plotted in the inset. Lower panel: photochemical evolution of acetone in a Cr-10 TUD-1 sample (black points) and a Cr-1 TUD-1 sample (gray points) exposed to 2.8 mbar of propane gas (time < 135 min), then 2.8 mbar of propane mixed with 400 mbar oxygen (time > 135 min), under blue light (475 nm, 18 mW/cm$^2$). Cr-1 TUD-1 is more efficient, so its scale has been compressed by a factor of 2.

dominated by the C═O stretching vibration of acetone (1669 cm$^{-1}$), which is well separated from the corresponding mode in carboxylates (1573 cm$^{-1}$). Between these is a third, poorly resolved band. Its position corresponds to the bending mode of adsorbed water (1635 cm$^{-1}$, reference spectra not shown). In the inset to Figure 3 the areas of these three bands, deconvoluted, are plotted as a function of time for a typical run.

The initial photo-oxidation rate is not sensitive to the presence of oxygen gas. Without oxygen gas, however, the rate decreases rapidly. This is illustrated in the lower panel of Figure 3. Here the radiometric density of acetone molecules is plotted as a function of irradiation time (475 nm, 18 mW/cm$^2$). In the first period the reagent gas is pure propane, and a gradual decrease of the photochemical oxidation rate is evident. At 135 min the propane has been replaced by an equivalent partial pressure of propane mixed with oxygen. The photochemical reaction rate increases, and this rate is sustained longer than in the absence of oxygen. Also shown is the result for Cr-1 TUD-1, which,

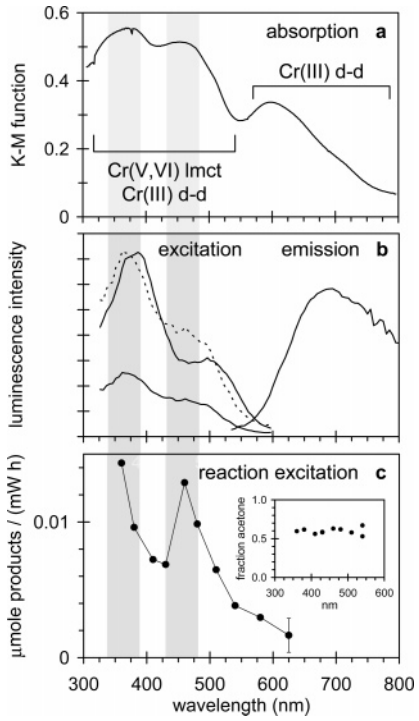


**Figure 4.** Electronic spectra of the Cr-10 TUD-1 sample. (a) Diffuse reflectance plotted as the Kubelka−Munk function, with regions of typical Cr ion absorption indicated (see text). (b) Luminescence spectrum under high vacuum (right-hand trace), luminescence-excitation spectrum (detected at 700 nm) under high vacuum (upper solid left-hand trace), and luminescence-excitation spectrum with reagents present (lower solid left-hand trace); the latter has also been scaled up facilitate comparison (broken line). (c) Initial propane oxidation rate as a function of excitation wavelength with an inset showing the molar fraction of $C_3$ product that is acetone. Shaded wavelength regions indicate the lmct absorptions of Cr(VI) oxide.

under identical circumstances, yields a larger number of product molecules. This material contains only 1 at % Cr/Si and no $Cr_2O_3$ inclusions.[6] The absorbed power is comparable because both samples are opaque at the excitation wavelength. Therefore the bulk photochemical yield on an absorbed-power basis is greater in Cr-1 TUD-1. A comparison of the moleuclar photochemical quantum yields is not justified, however, since the depth profiles of excitation intensity will differ. When rescaled as in Figure 3, the effect of oxygen gas on Cr-1 TUD-1 is proportionate to that observed in Cr-10 TUD-1.

Neither the initial photo-oxidation rate nor the selectivity are sensitive to the presence of oxygen in the feed. Clearly the reaction is not initiated by transfer of excitation from Cr to $O_2$, and the necessary oxygen atoms are sequestered directly from the catalyst. In the presence of oxygen gas, additional acetone is evidently produced via a Mars/van Krevelen redox chain: the catalyst itself is reduced, and in turn is reoxidized by the feed gas.

**Electronic Spectroscopy.** In Figure 4 three types of spectra are compared on a wavelength axis centered in the visible. The top panel is a diffuse-reflectance spectrum of Cr-10 TUD-1, obtained under ambient conditions, which has been plotted in the form of the Kubelka−Munk absorbance function. The sample certainly contains bulk chromium(III) oxide ($Cr_2O_3$) (as demonstrated in Figure 1). The oxide is responsible for both its olive-green appearance and the long-wavelength absorption features (580 nm and greater). These peaks are absent in TUD-1 samples doped with only 1% Cr, which contain no such crystalline inclusions (spectra not shown).[6] Although discrete absorbance maxima are evident in the short-wavelength region

of Figure 4a, these are difficult to assign because of the general congestion. Oxochromium species of valence III, V, and VI may be present, as all of these have electronic absorptions in this region.[12] The luminescence spectra shown in the middle panel of Figure 4 are somewhat simpler. Emission consists of a broad and featureless band with a maximum at 690 nm ("emission" trace). The intensity of this feature depends on excitation frequency, temperature, and the presence of reagents. The intensity of the emission peak as a function of pump frequency is also shown in Figure 4 ("excitation" traces). The stronger excitation spectrum was obtained under vacuum; the weaker trace was obtained at the same sensitivity with reagents present. This weakened emission has a slightly different spectral distribution than that observed under vacuum, as shown by the broken-line spectrum, which has been scaled up ($\times 2.9$) to facilitate comparison. Finally, the bottom panel of Figure 4 shows the dependence of the photo-oxidation rate on excitation wavelength. Each data point represents the initial rate of product formation in a fresh sample; the error bar indicates the magnitude of typical sample-to-sample variations. There is a general trend toward faster reaction at shorter wavelength. Superimposed on this is a maximum at approximately 460 nm.

The absorption feature at ~600 nm is characteristic of transitions centered on an octahedrally coordinated Cr(III) ion—specifically, between its occupied and unoccupied 2d orbitals.[13] The corresponding luminescence is expected in the near-infrared, at ~830 nm, beyond the range of Figure 4. Therefore the luminescence-excitation spectra in Figure 4b are simplified by virtue of being blind to chromium(III) oxide ($Cr_2O_3$). Both the broad emission feature at 690 nm and its excitation spectrum, with components at 380 and 500 nm, are characteristic of ligand-to-metal charge transfer (lmct) transitions in Cr(VI) oxides—compounds in which chromium is tetrahedrally bound to four oxygen atoms. The transitions correspond to the transfer of an electron from a nonbonding 2p orbital localized on oxygen to an antibonding 3d orbital of the chromium ion. The strong absorption at 380 nm is assigned to the symmetry-allowed transition $2e \leftarrow 4t_2$. The shoulder at 500 nm is generally attributed to $2e \leftarrow 1t_1$, which, although forbidden by the symmetry of these molecular orbitals, gains intensity from static or vibrational distortion of the tetrahedral bonding.[14] The result of photoactivation at these two wavelengths is a similar emitting state, which is supposed to be the lowest-lying triplet, populated via nonradiative relaxation.[15] On the basis of the general agreement in band positions and intensities, we follow these assignments for the emission−excitation spectra of Cr-10 TUD-1.

The various oxo-Cr(VI) species discussed in the literature have various degrees of distortion from tetrahedral symmetry. In model compounds it is observed that, in addition to the breaking of selection rules, such distortion shifts the absorption bands to lower energy.[16] On these grounds the apparent shift of the luminescence−excitation spectrum to higher energy when it is quenched by reagents (Figure 4b, broken line) may be interpreted as more efficient quenching of those oxo-chromium centers that are more distorted. These asymmetric sites are apparently more accessible to adsorbed gases or more reactive with them. Structural heterogeneity is certainly to be expected within the amorphous TUD-1 matrix, with the additional consequence that vibronic structure is not observable in the electronic spectra.

These assignments permit some interpretation of the reaction−excitation spectrum, Figure 4c. It is evident that d−d excitation of crystalline chromium(III) oxide ($Cr_2O_3$) does not contribute significantly to the photochemistry: the reaction rate is lowest when this transition exclusively is pumped at 620 nm. Insofar as this excitation is centered on the chromium ion and does not affect the bonding to oxygen ligands, the inactivity is not surprising. The very presence of Cr(V), in the form of, e.g., dichromate ions, is a matter of dispute,[17] but because the first lmct transition in this species peaks at 520 nm,[13] we can be confident that it too is not the principal agent of photochemical sensitization. The discrete reaction−excitation feature at 460 nm corresponds to the low-energy charge-transfer band of tetrahedrally coordinated Cr(VI). Such excitation does create a chemically reactive oxygen ligand. In the inset to Figure 4c the selectivity toward acetone is shown as a function of wavelength, as calculated at similar conversion levels for each point. Any dependence on excitation wavelength is weak, particularly in comparison to its strong effect on reaction rate. This is further evidence that the optically prepared state is not the one that initiates photo-oxidation. It has previously been reported that the reactivity of different oxides correlates with their triplet-state lifetimes, and on these grounds that the reactive species is the long-lived emitting state (triplet lmct).[18] Quenching of the emission by reagents, as observed here and in similar materials,[4] further support this conclusion.

Finally, we remark on the fact that luminescence quenching *efficiency* depends on excitation wavelength (a behavior that has previously been observed in chromium-doped HMS molecular seive[4]). This may be restated as: spectral inhomogeneity among the Cr(VI) centers correlates with their chemical accessibility to reagent gases, with the more distorted oxo-chromium centers being more easily quenched (Figure 4b). The excitation spectra that remain after quenching by oxygen alone or propane alone are similar, but whereas the luminescence is restored when oxygen is pumped away, the quenching by propane is irreversible. Together with the absence of a strong selectivity effect of either excitation wavelength or the presence of oxygen in the feed, the quenching behavior suggests that sensitization occurs between a partially relaxed chromophore and a propane molecule alone.

In conclusion, we have observed that the activity of a chromium-based photocatalyst depends strongly on excitation wavelength. The photochemical action spectrum is simpler than the linear absorption spectrum, and its structure corresponds to excitations of isolated Cr(VI) centers. Light absorbed by bulk Cr(III) oxide is wasted, making this catalyst composition less light efficient, but it has little effect on the chemical selectivity of the partial oxidation reactions that do occur. These observations are reasonably explained by the prevailing mechanistic hypothesis—that chemistry begins when a propane molecule encounters an accessible Cr(VI) site that is in a long-lived excited state. The heterogeneity of light-absorbing centers in this catalyst is characteristic of systems with a relatively high loading of the active phase. In this particular case wavelength selection can be used to investigate the photochemical mechanism and furthermore to optimize the photochemical efficiency without loss of selectivity. In contrast to conventional, thermally activated heterogeneous catalysis, the selectivity of the present photochemical system does not decrease strongly with increasing conversion. This suggests that carbonate species are formed directly from propane, rather than by a consecutive reaction with acetone. Additional details concerning the participation of triplet states, and the role of intermediate oxygenates, could in principle be obtained by the same spectroscopic methods if time-resolved.

**Acknowledgment.** S.T.W. is gratefully acknowledged for financial support. Prof. Dr. Ir. B. M. Weckhuysen is acknowledged for fruitful discussion.

## References and Notes

(1) Maldotti, A., Molinari, A., Amadelli, R. *Chem. Rev.* **2002**, *102*, 3811−3836.
(2) Frei, H. *Science* **2006**, *313*, 309.
(3) Yamashita, H.; Yoshizawa, K.; Ariyuki, M.; Higashimoto, S.; Che, M.; Anpo, M. *Chem. Commun.* **2001**, 435−436.
(4) Yamashita, H.; Ariyuki, M.; Yoshizawa, K.; Kida, K.; Ohshiro, S.; Anpo, M. *Res. Chem. Intermed.* **2004**, *30*, 235−245.
(5) Yamashita, H.; Ohshiro, S.; Kida, K.; Yoshizawa, K.; Anpo, M. *Res. Chem. Intermed.* **2003**, *29*, 881−890.
(6) Hamdy, M. S.; Berg, O.; Jansen, J. C.; Maschmeyer, T.; Arafat, A., Moulijn, J. A.; Mul, G. *Catal. Today* **2006**, *117*, 337−342.
(7) Hamdy, M. S.; Berg, O.; Jansen, J. C.; Maschmeyer, T.; Moulijn, J. A.; Mul, G. *Chem.−Eur. J.* **2005**, *12*, 620−628.
(8) Barrett, E. P.; Joyner, L. G.; Halenda, P. P. *J. Am. Chem. Soc.* **1951**, *73*, 373−380.
(9) Lippens, B. C.; de Boer, J. H. *J. Catal.* **1965**, *4*, 319−323.
(10) Matyshak, V. A.; Krylov, O. V. *Kinet. Catal.* **2002**, *43*, 391−407.
(11) Jansen, J. C.; Shan, Z.; Marchese, L.; Zhou, W.; von der Puil, N.; Maschmeyer, T. *Chem. Commun.* **2001**, 713−714.
(12) Lever, A. B. P. *Inorganic Electronic Spectroscopy*, 2nd ed; Elsevier: 1984.
(13) Weckhuysen, B. M.; Wachs, I. E.; Schoonheydt, R. A. *Chem. Rev.* **1996**, *96*, 3327−3349.
(14) Johnson, L. W.; McGlynn, S. P. *Chem. Phys. Lett.* **1970**, *7*, 618−620.
(15) Hazenkamp, M. F.; Blasse, G. *J. Phys. Chem.* **1992**, *96*, 3442−3446.
(16) Dalhoeven, G. A. M.; Blasse, G. *Chem. Phys. Lett.* **1980**, *76*, 27−29.
(17) Groppo, E.; Lamberti, C.; Bordiga, S.; Spoto, G.; Zecchina, A. *Chem. Rev.* **2005**, *105*, 115−183.
(18) Anpo, M.; Tanahashi, I.; Kubokawa, Y. *J. Phys. Chem.* **1982**, *86*, 1−3.